Heliyon 10 (2024) e24868

Contents lists available at ScienceDirect

Heliyon

journal homepage: www.cell.com/heliyon

Research article

Virtual screening, activity evaluation, and stability of pancreatic lipase inhibitors in the gastrointestinal degradation of nattokinase

Lina Yang [a,b], Shufang Cao [b], Mengxi Xie [a], Taiyuan Shi [a,*]

[a] Food and Processing Research Institute, Liaoning Academy of Agricultural Sciences, Shenyang, Liaoning, 110161, China
[b] College of Food Science and Engineering, Bohai University, Jinzhou, Liaoning, 121013, China

ARTICLE INFO

Keywords:
Nattokinase
Pancreatic lipase
Virtual screening
Molecular docking
Molecular dynamics

ABSTRACT

Nattokinase is an alkaline serine protease secreted by natto during fermentation. Despite its good thrombolytic effect, it is intolerant to gastrointestinal conditions and is easily digested and degraded into polypeptides, oligopeptides, and amino acids. However, whether these peptides inhibit fat-digesting enzymes and other biological activities remains unknown. To explore the bioactivity of peptides produced through nattokinase degradation, nattokinase was subjected to simulated digestion in the gastrointestinal tract, and 41 small peptides were obtained through the enzymolysis of gastric enzymes, pancreases, and chymotrypsin. Four pancreatic lipase (PL) inhibitory peptides (SW, ASF, GAY, and PGGTY) were selected based on their activity scores, water solubility, and toxicity predictions. The molecular docking results revealed that hydrogen bonds and electrostatic interactions were the main forces for inhibiting PL activity. The results of enzyme activity verification revealed that all four peptides inhibited PL activity. Among them, GAY exhibited the strongest inhibitory effect, with an inhibitory rate of 10.93 % at a concentration of 1 mg/mL. Molecular dynamics simulations confirmed that the GAY–1ETH complex demonstrated good stability. Natto foods containing nattokinase own the activity of inhibiting fat-digesting enzymes and show antiobesity potentials.

1. Introduction

Obesity refers to a state of being noticeably overweight and the fat layers being too thick owing to the accumulation of body fat, especially triglycerides [1,2]. According to the China Office of the International Society for Life Sciences, in China, a body mass index of ≥28 is considered obese [3]. The process of fat absorption and metabolism in the body mainly involves the participation of the tongue, gastric, and pancreatic lipases [4,5]. Among them, pancreatic lipase (PL) is the most important and extensively studied potential target for obesity treatment. PL is the major lipolytic enzyme synthesized and secreted for the pancreas, and the catalytic hydrolysis of fats into glycerol and fatty acids plays a key role [6]. Free fatty acids produced in this process can be absorbed and reused in the body to synthesize fat. Therefore, inhibiting PL can reduce fat decomposition, leading to decreased absorption of body fat, which helps control obesity. Finding effective substances to inhibit PL activity is an important means of managing obesity.

Chemical synthetic antiobesity drugs often have several side effects, such as gastrointestinal tract and neuronal damage [7]. Researchers are constantly exploring natural and safer alternatives, mostly phytochemicals and food-derived molecules [8–11]. Peptides

* Corresponding author. Food and Processing Research Institute, Liaoning Academy of Agricultural Sciences. Dongling Road No.84, Shenyang, Liaoning, 110161, China.
E-mail addresses: yangln10@lzu.edu.cn (L. Yang), 326595539@qq.com (T. Shi).

https://doi.org/10.1016/j.heliyon.2024.e24868
Received 23 October 2023; Received in revised form 13 January 2024; Accepted 16 January 2024
Available online 17 January 2024

derived from food proteins reportedly reduce oxidative stress and inflammation as well as inhibit enzymes such as lipase and α-amylase [12–14]. In recent years, computer-aided screening of active peptides has been increasingly studied [15–17]. Using online data and virtual screening methods reduces work intensity, labor costs, and the research and development cycle and improves the success rate of identifying active peptides. Consequently searching for potential PL inhibitors through molecular docking and virtual screening is feasible.

Nattokinase, or hay Bacillus protease, is a serine protease produced during natto fermentation by Bacillus subtilis natto [18,19]. It comprises 275 amino acids arranged in a fixed sequence, and its molecular weight is 27.7 kDa [20]. Nattokinase is known for its ability to dissolve thrombus, reduce blood viscosity, improve blood circulation, soften blood vessels, and increase blood vessel elasticity, among others [21–23]. When ingested, it is easily digested and degraded into peptides, oligopeptides, and amino acids under the action of gastric acid, bile salts, and certain protein kinases [22]. However, the biological activity of these enzymolytic peptides remains unknown. Therefore, herein, the biological activity, water solubility, and hepatotoxicity of enzymatic hydrolyzed peptides of nattokinase were predicted using online databases. Additionally, the PL inhibitory activity of these peptides was explored through molecular docking and *in vitro* experiments.

2. Results and discussion

2.1. Virtual enzymolysis of nattokinase

Nattokinase was subjected to simulated gastrointestinal tract digestion using pepsin, trypsin, and chymotrypsin. Subsequently, 64 peptides were screened, comprising 23 amino acids and 41 peptide segments (Table 1). The 41 peptide segments included four dipeptides, six tripeptides, six tetrapeptides, four pentapeptides, and 21 6-peptides or above. The bioactivity prediction scores of the dipeptide SW, tripeptides ASF and GAY, tetrapeptides HPTW and APAL, and pentapeptide PGGTY exceeded 0.5, indicating their potential high bioactivity.

2.2. Virtual screening of pancreatic lipase–inhibiting peptides

ADMET, which involves a comprehensive study of drug absorption, distribution, metabolism, excretion, and toxicity, can be used to identify bioactive peptides with *in vivo* activity and is a crucial method in contemporary drug design and screening [24]. Water solubility considerably impacts bioactive peptide absorption, as solubility is the limiting factor for the physiological functions of bioactive peptides [25]. The six selected peptides—SW, ASF, GAY, HPTW, APAL, and PGGTY—exhibited good water solubility (Table 2). The two tetrapeptides, HPTW and APAL, were hepatotoxic, while the remaining four peptides, SW, ASF, GAY, and PGGTY, demonstrated no hepatotoxicity, indicating their reduced potential harm to the human body.

The above screening peptides were searched in BIOPEP-UWM (https://biochemia.uwm.edu.pl/biopep-uwm/) and online database. SW was identified as a dipeptide peptidase inhibitor and can facilitate the recovery of intestinal function, promote pancreatic hormone release, stimulate insulin secretion, suppress appetite, and reduce food intake. ASF, GAY, and PGGTY were not selected and were presumed to be lipase activity inhibitors.

Based on the activity scores and ADMET prediction results, four peptides (SW, ASF, GAY, and PGGTY) were selected as PL inhibitory peptides. Subsequent *in vitro* experiments were conducted to verify their inhibitory activity. The chemical structures (StoneMIND Collector, StoneWise, Beijing, China) of these four peptides are shown in Fig. 1C.

2.3. Molecular docking of potential peptides and pancreatic lipase

2.3.1. Interaction force

The CDOCKER scoring function, specifically "-CDOCKER_INTERACTION_ENERGY," was employed. The lowest -CDOCKER_INTERATION_ENERGY value was selected from the 10 conformations generated by docking each polypeptide with PL. The minimum

Table 1
Nattokinase Simulation results of gastrointestinal digestion *in vitro* and activity score.

Peptide sequence	Activity score	Peptide sequence	Activity score	Peptide sequence	Activity score	Peptide sequence	Activity score
SW	0.93	HPTW	0.81	AISNNM	0.30	IINGIEW	0.33
GK	0.30	APAL	0.61	AQSVPY	0.24	AAGTIAA	0.19
DR	0.29	SQGY	0.40	GISQIK	0.18	GVAPSAS	0.15
SK	0.07	GGAS	0.29	NNSIGV	0.18	VPSETNPY	0.20
ASF	0.77	ATPH	0.24	QDGSSH	0.15	GGPTGSTA	0.19
GAY	0.55	YAVK	0.09	VAGAAA	0.12	DSTGSGQY	0.14
DVM	0.28	PGGTY	0.54	SSVGSE	0.09	INVQAAAQ	0.06
GTH	0.20	NGTSM	0.25	TNAQVR	0.08	APGVSIQSTL	0.25
GNS	0.20	DVINM	0.23	ESTATY	0.07	VAVIDSGIDSSHPDL	0.15
NVR	0.09	TVVDK	0.03	TGSNVK	0.06	YPSTIAVGAVNSSNQR	0.17
						AVSSGIVVAAAAGNEGSSGSTSTVGYPAK	0.41

Table 2
Solubility and toxicity prediction of nattokinase peptides (activity score > 0.5).

Peptide sequence	Solubility level	Hepatotoxic prediction
SW	5	False
ASF	5	False
GAY	5	False
HPTW	4	True
APAL	5	True
PGGTY	5	False

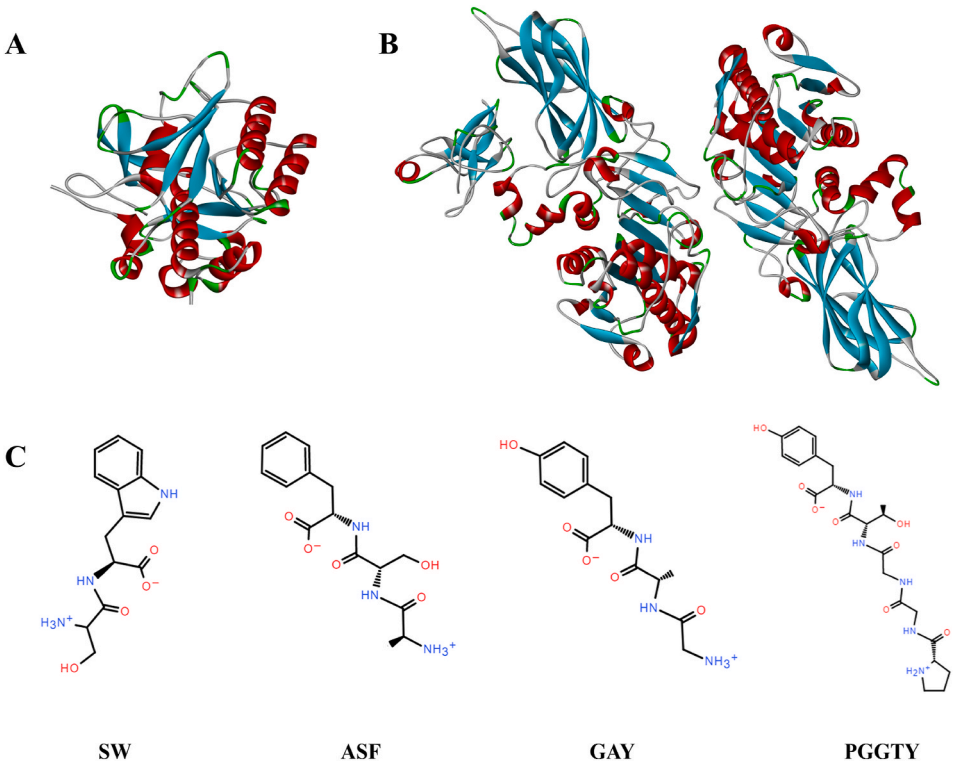

Fig. 1. Chemical structures of nattokinase, pancreatic lipase and peptides. (A) Crystal structure of nattokinase. (B) Crystal structure of pancreatic lipase. (C) Chemical structures of four nattokinase peptides screened by virtual hydrolysis.

docking scores for SW, ASF, GAY, and PGGTY in 1ETH were 52.557, 60.2097, 57.8884, and 79.9242 kcal/mol, respectively. The complex with the closest binding mode among the 10 conformations was selected.

The dipeptide SW had hydrogen bond interactions with the amino acids GLU188, ARG191, PRO194, and SER323 in 1ETH, as well as hydrophobic interactions with VAL322 and charge interactions with GLU188, ARG191, and ASP193 (Fig. 2A). The tripeptide ASF had a hydrogen bond interaction with the amino acids GLU188, ARG191, PRO194, GLN220, and THR221 in 1ETH; a charge interaction with Glu188, ARG191, and ASP193; and a hydrophobic interaction with PRO187 (Fig. 2B). The tripeptide GAY had hydrogen bond interactions with the amino acids GLU188, PRO194, GLN220, THR221, and VAL222 in 1ETH and charge interactions with GLU188 and ARG191 (Fig. 2C). The pentapeptide PGGTY had hydrogen bond interactions with the amino acids ARG164, GLU188, Arg191, Pro194, GLN220, and SER323 in 1ETH; charge interactions with GLU188 and ASP193; and hydrophobic interactions with LEU189. However, it formed unfavorable bonds with GLU188 and ARG191 (Fig. 2D).

The molecular docking results showed that SW, ASF, GAY, and PGGTY primarily had hydrogen bond interactions with the amino acids ARG164, GLU188, ARG191, PRO194, GLN220, THR221, VAL222, and SER323 in 1ETH. They had a hydrophobic interaction with the amino acids PRO187, LEU189, and VAL322; a charge interaction with the amino acids GLU188, ARG191, and ASP193; and unfavorable binding with GLU188 and ARG191. The hydrogen bond was the main force between the peptides and 1ETH. SW, ASF, GAY, and PGGTY had hydrogen bond interactions with four, five, five, and six amino acids in 1ETH, respectively. Peptides from cow casein hydrolysate (MMML, FDML, and HLPGRG) and camel casein hydrolysate (AAGF, MSNYF, and FLWPEYGAL) have been identified as potential inhibitors of PL [26]. In another study, PL inhibitory peptides were prepared from the protein hydrolysates of sea buckthorn seed meal [27], where EEAASLR, FR, NLLHR, APYR, RDR, and VR were identified as potential antiobesity peptides. The interaction between these six peptides and PL involved various mechanisms, including hydrophilic interaction, hydrogen bonding,

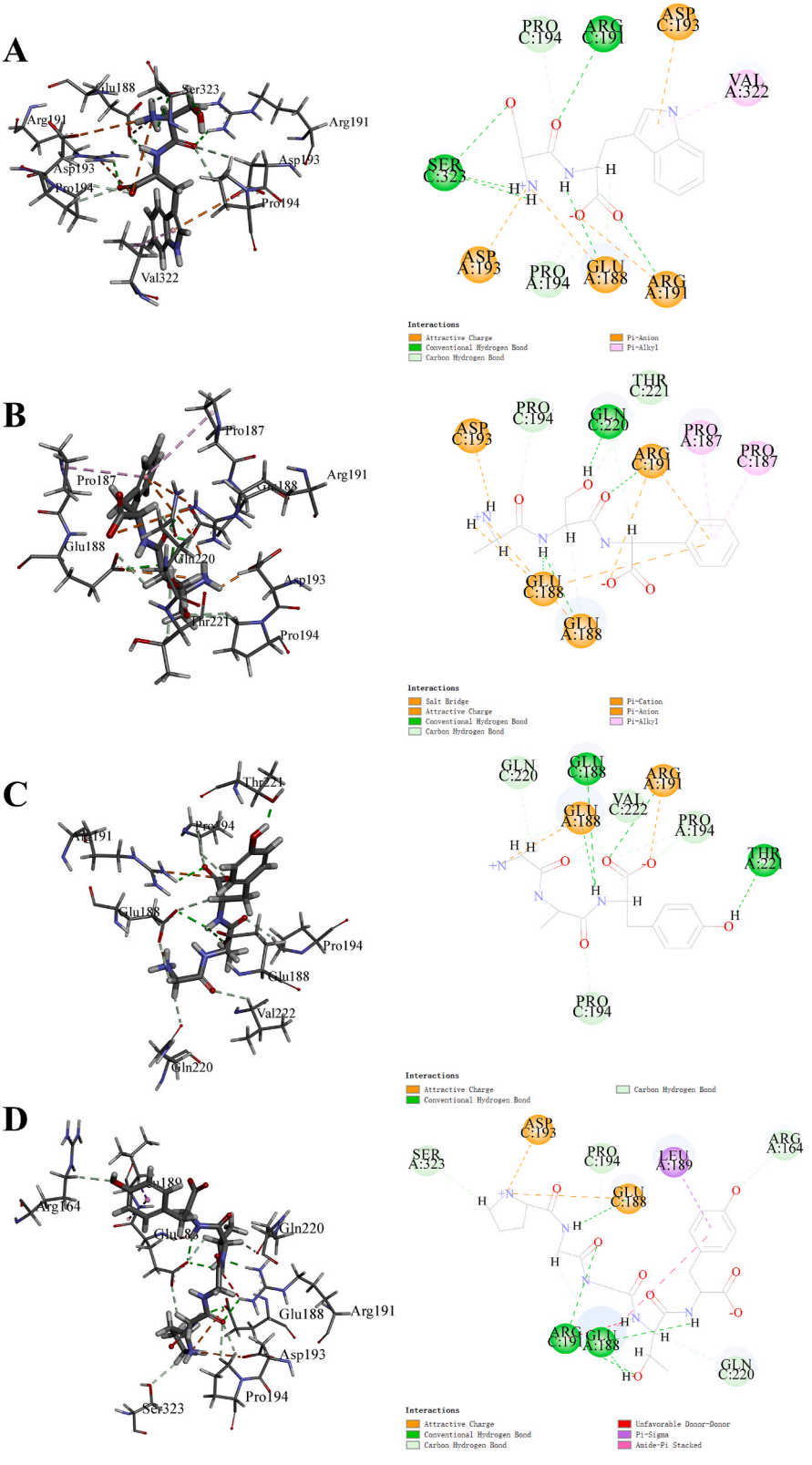

1

(caption on next page)

Fig. 2. Interaction force and site between peptides and 1ETH with molecular docking. (A) Interaction force and site between SW and 1ETH with molecular docking. (B) Interaction force and site between ASF and 1ETH with molecular docking. (C) Interaction force and site between GAY and 1ETH with molecular docking. (D) Interaction force and site between PGGTY and 1ETH with molecular docking.

hydrophobic interaction, and π–π interaction.

2.3.2. Heat map of hydrogen bonds

In Fig. 3A, nine hydrogen bonds were observed between GLU188 and SW in chain A, while eight were observed between GLU188 and SW in chain C. Nine hydrogen bonds were observed between GLU188 (A), GLU188 (C), and ASF, while eight were observed between VAL222 (A), PRO194 (C), and ASF (Fig. 3B). Similarly, nine hydrogen bonds were observed between ARG191 (A), GLU188 (C), and GAY, while eight were observed between THR221 (A) and GAY (Fig. 3C). Nine hydrogen bonds were observed between GLU188 (A), THR221 (C), and PGGTY. Furthermore, 10 hydrogen bonds were observed between GLU188 (C) and PGGTY, while eight were observed between SER323 (C) and PGGTY (Fig. 3D). The amino acid residues GLU188 (A), ARG191 (A), GLU188 (C), and PRO194 (C) in 1ETH were observed to be crucial in peptide binding (Fig. 3E). In addition, the number of hydrogen bonds between PGGTY and 1ETH was significantly higher than that observed between SW, ASF, and GAY.

2.4. Inhibition activity of pancreatic lipase

Inhibiting PL is an effective method for treating obesity. Many studies have investigated the potential efficacy of food bioactive compounds, such as antiobesity molecules, by inhibiting PL. To verify the accuracy of virtual screening, a PL inhibitory activity assay was conducted for four peptides, which showed dose-dependent PL inhibition (Fig. 4A). All four peptides partially inhibited lipase activity. With an increase in peptide concentration, the inhibitory effect of the extract on lipase increased within a certain concentration range. At a certain concentration level, the inhibition rate decreased. Fig. 4 A&B shows that GAY exhibited the strongest inhibitory effect on PL, with an inhibitory rate of 10.93 % at a concentration of 1 mg/mL, followed by SW. PGGTY exhibited the least inhibitory effect on PL, possibly due to unfavorable binding interactions with GLU188 and ARG191, when it binds to amino acid residues in the binding site. In a previous study, peptides consisting of up to 21 amino acid residues from cumin seeds reduced lipase activity by 22.6 %–54.6 % at 2.5 mg/mL concentrations [28].

2.5. Stability of the potential peptide and pancreatic lipase

Molecular dynamics simulations were conducted to explore the interaction between GAY and 1ETH based on GAY exhibiting the strongest inhibitory effect on PL *in vitro*. During the molecular dynamics simulation, the total, potential, and kinetic energy levels were monitored (Fig. 5A). Notably, in the kinetic simulation, the three energies remained stable from 0 to 100 ns, indicating that the system simulation was stable. The energy composition of the binding free energy is shown in Fig. 5B. The most significant favorable contributions to GAY binding with 1ETH stemmed from van der Waals and electrostatic energies. Conversely, polar solvation free energy was largely unfavorable. However, van der Waals and electrostatic energies can counteract the negative effects of polar solvation free energy, thereby facilitating binding.

Fig. 5C illustrates the binding composition of the GAY–1ETH complex before and after 100 ns of simulation, showing changes in the ligand conformation. Root mean square deviation (RMSD) measures conformational differences from a reference molecule and can be used to rapidly determine whether the trajectory has reached equilibrium [29–31]. Fig. 5D shows a “plateau” in the RMSD value between 40 and 100 ns of the simulated trajectory, indicating that GAY was stably bound to 1ETH and that the protein structure tended to be stable. Root mean square fluctuation (RMSF) is primarily used to illustrate the range of structural changes in each residue during the simulation (sequence segments with high RMSF values are highly flexible) [32]. Fig. 5E shows that the average RMSF value of the entire receptor system is 1.90 Å, with the largest fluctuation observed for isoleucine 249 (~7.49 Å). The RMSF values for the key residues of GAY interacting with 1ETH are relatively low, with an average value of ~1.52 Å. This result indicates that the key residues have reduced flexibility and maintain stable binding owing to the interaction between the 1ETH receptor and the GAY ligand. The radius of gyration (Rg) characterizes the tightness of protein molecules [33]. Some studies have shown that changes in the Rg value are negatively correlated with the compactness of the material structure [34]. The Rg value of the receptor exhibits an overall downward trend from 0 to 40 ns, followed by a gradual increase from 40 to 100 ns, eventually stabilizing around 35 Å (Fig. 5F). Fig. 5G shows the trace of the solvent accessibility surface area (SASA) for the ligand. The figure shows that the trace of the ligand SASA fluctuates significantly, with an average value of ~68.20. This may be because of the binding of GAY with 1ETH, resulting in conformational changes in the ligand. Consequently, the SASA trajectory of the ligand fluctuates significantly. Molecular dynamics simulations confirmed the good stability of the GAY–1ETH complex.

3. Conclusions

Four good water-soluble and nontoxic peptides, SW, ASF, GAY, and PGGTY, were screened through virtual the enzymatic digestion of nattokinase for molecular docking with 1ETH. The molecular docking results revealed that hydrophobic, charge, and hydrogen bond interactions were crucial in the interaction between these peptides and PL. The activity tests revealed that all four peptides inhibited PL to some extent. Moreover, the results of the molecular dynamics simulations confirmed the good stability of the GAY–1ETH complex,

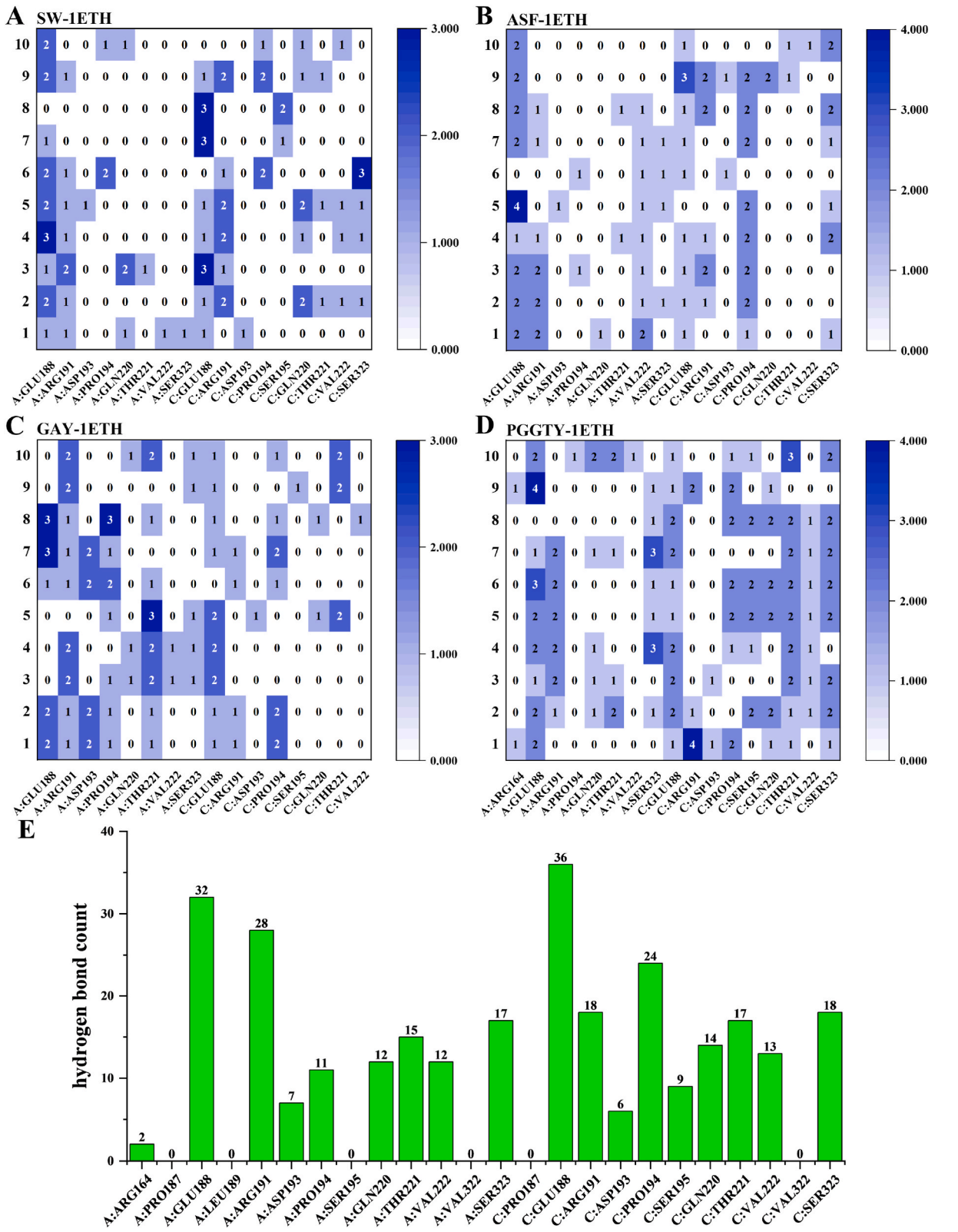

Fig. 3. The number of hydrogen bonds between peptides and 1ETH. (A) The number of hydrogen bonds between SW and 1ETH. (B) The number of hydrogen bonds between ASF and 1ETH. (C) The number of hydrogen bonds between GAY and 1ETH. (D) The number of hydrogen bonds between PGGTY and 1ETH. (E) The count of hydrogen bonds of 1ETH with SW, ASF, GAY and PGGTY.

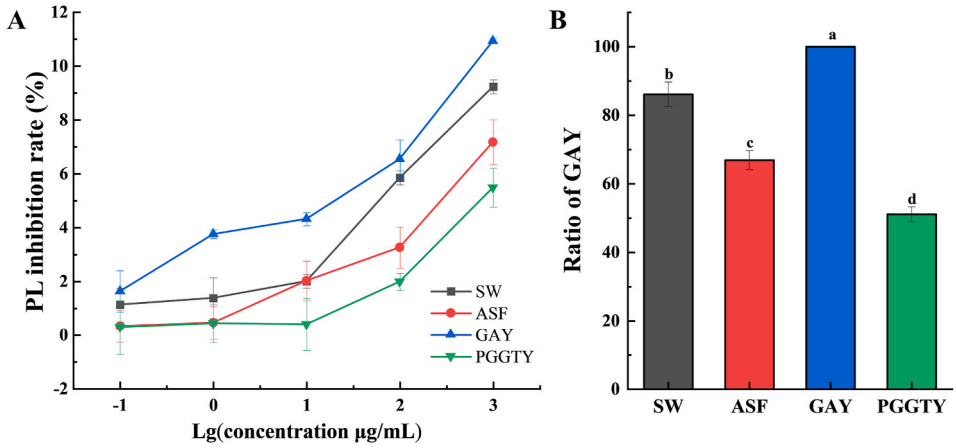

Fig. 4. The inhibitory effect of peptides on pancreatic lipase. (A) The inhibition rate. (B) Ratio of inhibition rate.

suggesting that GAY could serve as an antiobesity peptide. Therefore, natto foods containing nattokinase offer certain antiobesity effects, expanding their potential applications.

4. Materials and methods

4.1. Virtual enzymatic digestion of nattokinase

Nattokinase-related protein sequences were retrieved from the UniProt database, and a nattokinase · Bacillus subtilis (A2TJV0 · A2TJV0_BACIU) containing 275 amino acids was selected (Fig. 1A). Virtual hydrolysis of nattokinase was conducted with the Expasy Peptide Cutter (https://web.expasy.org/peptide_cutter/) program using proteases such as pepsin (pH 1.3) (EC 3.4.23.1), trypsin (EC 3.4.21.4), and chymotrypsin (EC 3.4.21.1). Subsequently, multiple peptide sequences were obtained.

4.2. Biological activity score

All the peptide sequences obtained by virtual hydrolysis were conducted for bioactivity prediction in the PeptideRanker program. Active peptides with a biological activity score of 0.5 or higher were selected.

4.3. Prediction of pharmacokinetics

The peptides screened in Section 4.2 were imported into the Discovery Studio (DS) 2017 R2 software. The pharmacokinetic descriptors (absorption, distribution, metabolism, excretion, and toxicity (ADMET)) were accessed in the DS software's toolbar. After selecting all the peptides, the ADMET properties to be predicted (water solubility and hepatotoxicity) were selected, and the prediction results were recorded and analyzed.

4.4. Molecular docking

The 3D structures were constructed of the previously identified active peptides obtained through virtual enzymatic hydrolysis as ligands using the DS Client. The active peptides were optimized under the CHARMm force field to minimize their energy. The crystal structure of PL (PDB: 1ETH) (Fig. 1B) was downloaded from the RCSB PDB (https://www.rcsb.org/) database. Before molecular docking, corresponding structural treatments were applied, including the removal of water molecules, the addition of incomplete amino acid residues, the hydrogenation of atoms, and the setting of receptor binding sites. The docking of the PL and active peptides was conducted using the CDOCKER module of the DS software. PL was defined as a receptor, and potential binding sites were searched. Molecular docking was performed using the CDOCKER docking program in Dock Ligands, generating 10 docking conformations per molecule. At this point, the coordinates of the cavity where the peptides interact with PL are X = 72.125, Y = 36.946, Z = 145.178, and the radius of the cavity is 20. The data were screened after the results were obtained, and the interaction between the polypeptides and PL was analyzed to generate a hydrogen bond heat map.

4.5. Evaluation of pancreatic lipase inhibitory activity

PL (Shanghai yuanye Bio-Technology Co., Ltd.) inhibitory activity assays were conducted following the method of Zhang et al. [35, 36] with slight modifications. This involved mixing 200 μL of the sample—1 mg/mL active peptide (Shanghai, Sangon Biotech Co., Ltd.) solution— with 45 μL of a 1 mg/mL PL solution in 0.1 mol/L Tris-HCl buffer. After incubation at 37.0 °C for 20 min, 100 μL of 11

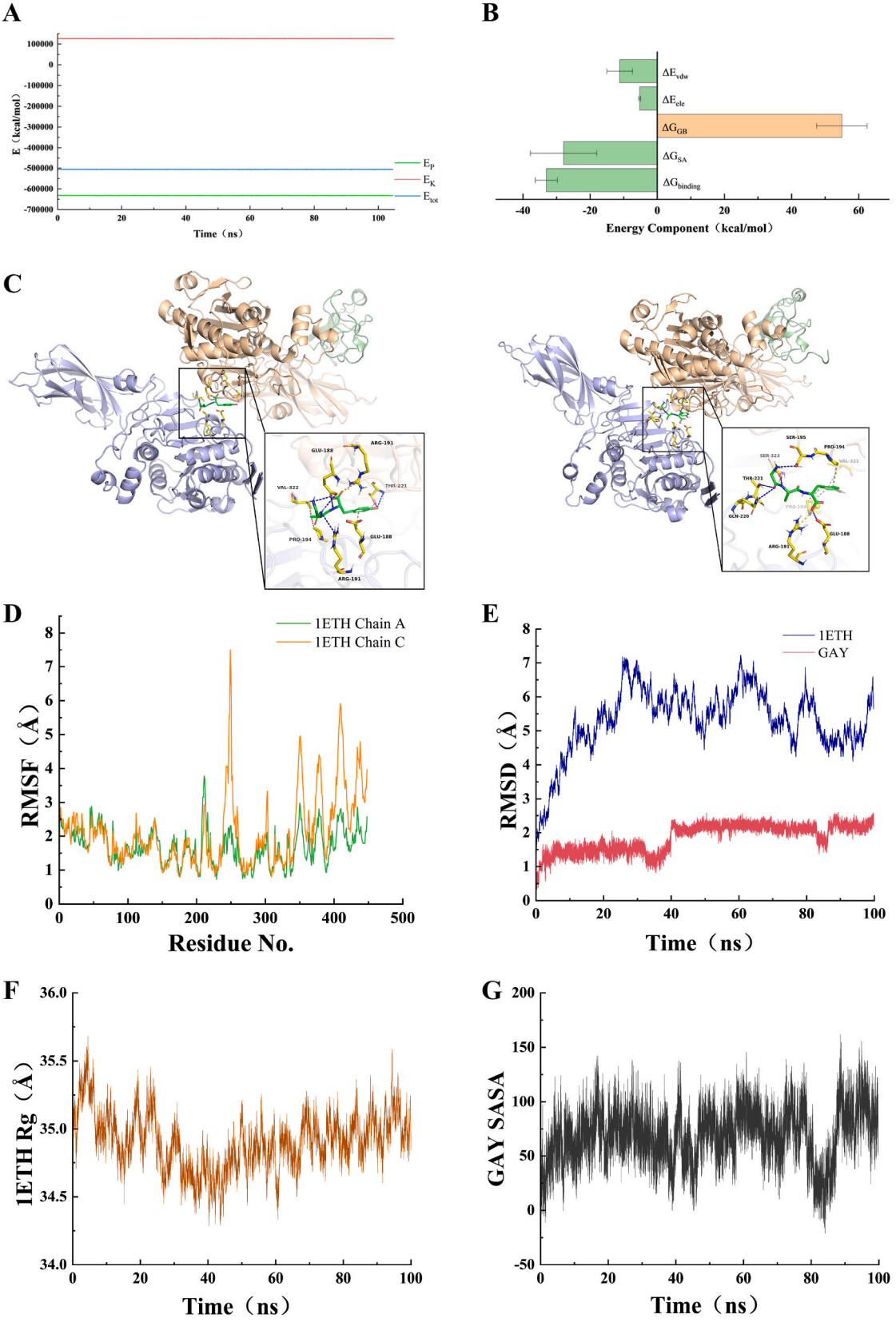

(caption on next page)

Fig. 5. Molecular dynamic simulation of GAY and 1ETH. (A) Molecular dynamic simulation of 0∼100 ns energy curve of GAY and 1ETH. (B) Binding free energy of GAY and 1ETH during the simulation. (C) Conformational changes of GAY and 1ETH complexes before and after molecular simulation. (D) RMSD at 0–100 ns. (E) RMSF at 0–100 ns. (F) Rg at 0–100 ns. (G) SASA at 0–100 ns.

mmol/L *p*-NPB (HeFei BoMei Biotechnology Co.,Ltd) was added to obtain a final volume of 1000 μL. The reaction mixture was allowed to react at 37.0 °C for 15 min and then terminated by placing it in boiling water for 10 min. Subsequently, 200 μL of the reaction mixture was added to a 96-well plate, and the absorbance value was measured at a wavelength of 405 nm using a microplate reader (PerkinElmer, USA, ELX-800UV). The inhibitory activity was calculated using the following formula:

$$\text{Enzyme inhibition} = \left(1 - \frac{A_{\text{sample}} - A_{\text{sample blank}}}{A_{\text{control}} - A_{\text{control blank}}}\right) \times 100\% \quad (1)$$

4.6. Molecular dynamics simulation

The FF99SB force field of the Amber18 program was used to describe the target protein residues and tripeptide structures. The tripeptide molecules and target protein complex structures obtained from molecular docking were placed in an octahedral periodic boundary solvent box filled with TIP3P water. The minimum distance from the complex surface to the box was 10 Å. After the geometry of the complex system was optimized and the temperature of the system was gradually heated from 0 K to 298 K, the sander module of the Amber 18 program was used to model the complex structure of the polypeptides and the target protein at T = 298 K. The binding free energy of the complex was calculated using the MM/GBSA method to evaluate the binding ability of the polypeptides to the target proteins.

4.7. Statistical analysis

Experimental data are presented as mean ± SD. Origin 2022 was used for mapping. All experiments and analyses were repeated at least three times.

Data statements

The data that support the findings of this study are available on request from the corresponding author.

CRediT authorship contribution statement

Lina Yang: Writing – review & editing, Software, Methodology, Formal analysis, Data curation, Conceptualization. **Shufang Cao:** Writing – original draft, Formal analysis, Data curation. **Mengxi Xie:** Resources, Methodology, Conceptualization. **Taiyuan Shi:** Supervision, Resources, Methodology, Conceptualization.

Declaration of competing interest

The authors declare that they have no known competing financial interests or personal relationships that could have appeared to influence the work reported in this paper.

Acknowledgements

Thanks for the Liaoning Province “Jie Bang Gua Shuai” Science and Technology Research Project (2021JH1/1040003402).

References

[1] Z. Dong, L. Wu, Y. Chen, O. Lyulyov, T. Pimonenko, Intergenerational transmission of obesity: role of education and income, Int. J. Environ. Res. Publ. Health 19 (23) (2022) 15931.
[2] S. Cao, L. Yang, M. Xie, M. Yu, T. Shi, Peanut-natto improved obesity of high-fat diet mice by regulating gut microbiota and lipid metabolism, J. Funct. Foods 112 (2024) 105956.
[3] C. Chen, Overview of obesity in mainland China, Obes. Rev. 9 (2008) 14–21.
[4] T. Liu, T. Liu, X. Chen, Y. Shi, Lipase inhibitors for obesity: a review, Biomed. Pharmacother. 128 (2020) 110314.
[5] P. Wang, D. Wan, T. Peng, Y. Yang, X. Wen, X. Yan, J. Xia, Q. Zhu, P. Yu, D. Gong, Acute oral toxicity and genotoxicity test and evaluation of cinnamomum camphora seed kernel oil, Foods 12 (2) (2023) 293.
[6] A. Kumar, S. Chauhan, Pancreatic lipase inhibitors: the road voyaged and successes, Life Sci. 271 (2021) 119115.
[7] H. Aldewachi, Y.F. Mustafa, R. Najm, F. Ammar, Adulteration of slimming products and its detection methods, Sys. Rev. Pharm. 11 (3) (2020) 289.
[8] G.A. Mohamed, S.R. Ibrahim, E.S. Elkhayat, R.S. El Dine, Natural anti-obesity agents, Bull. Fac. Pharm. Cairo Univ. 52 (2) (2014) 269–284.
[9] S. Zhang, L. Yang, Y. Nie, H. Liu, D. Zhu, Research progress on the effect of cooking and freezing processes on the quality of frozen dough steamed buns, Int. J. Food Eng. 24 1 (2024) 1–15.
[10] L. Yang, X. Wu, M. Luo, T. Shi, F. Gong, L. Yan, J. Li, T. Ma, R. Li, H. Liu, $Na^+/Ca^{2}+$ induced the migration of soy hull polysaccharides in the mucus layer *in vitro*, Int. J. Biol. Macromol. 199 (2022) 331–340.
[11] X. Wu, L. Yang, M. Xia, K. Yu, W. Cai, T. Shi, M. Xie, H. Liu, Na^+/K^+ enhanced the stability of the air/water interface of soy hull polysaccharide and intestinal mucus, Int. J. Biol. Macromol. 245 (2023) 125206.

[12] R. Esfandi, I. Seidu, W. Willmore, A. Tsopmo, Antioxidant, pancreatic lipase, and alpha-amylase inhibitory properties of oat bran hydrolyzed proteins and peptides, J. Food Biochem. 46 (4) (2022) e13762.
[13] N. Rodríguez-Arana, K. Jiménez-Aliaga, A. Intiquilla, J.A. León, E. Flores, A.I. Zavaleta, V. Izaguirre, C. Solis-Calero, B. Hernández-Ledesma, Protection against oxidative stress and metabolic alterations by synthetic peptides derived from Erythrina edulis seed protein, Antioxidants 11 (11) (2022) 2101.
[14] R. Vilcacundo, C. Martínez-Villaluenga, B. Hernández-Ledesma, Release of dipeptidyl peptidase IV, α-amylase and α-glucosidase inhibitory peptides from quinoa (Chenopodium quinoa Willd.) during *in vitro* simulated gastrointestinal digestion, J. Funct.Foods 35 (2017) 531–539.
[15] M.H. Cardoso, R.Q. Orozco, S.B. Rezende, G. Rodrigues, K.G. Oshiro, E.S. Cândido, O.L. Franco, Computer-aided design of antimicrobial peptides: are we generating effective drug candidates? Front. Microbiol. 10 (2020) 3097.
[16] C. Wen, J. Zhang, H. Zhang, Y. Duan, H. Ma, Plant protein-derived antioxidant peptides: isolation, identification, mechanism of action and application in food systems: a review, Trends Food Sci. Technol. 105 (2020) 308–322.
[17] M.O. Idris, A.A. Yekeen, O.S. Alakanse, O.A. Durojaye, Computer-aided screening for potential TMPRSS2 inhibitors: a combination of pharmacophore modeling, molecular docking and molecular dynamics simulation approaches, J. Biomol. Struct. Dyn. 39 (15) (2021) 5638–5656.
[18] L. Yuan, C. Liangqi, T. Xiyu, L. Jinyao, Biotechnology, bioengineering and applications of Bacillus nattokinase, Biomolecules 12 (7) (2022) 980.
[19] S. Ju, Z. Cao, C. Wong, Y. Liu, M.F. Foda, Z. Zhang, J. Li, Isolation and optimal fermentation condition of the Bacillus subtilis subsp. natto strain WTC016 for nattokinase production, Fermentation 5 (4) (2019) 92.
[20] S.-J. Kang, Y. Lim, A.-J. Kim, Korean red ginseng combined with nattokinase ameliorates dyslipidemia and the area of aortic plaques in high cholesterol-diet fed rabbits, Food Sci. Biotechnol. 23 (2014) 283–287.
[21] M. Milner, K. Makise, Natto and its active ingredient nattokinase: a potent and safe thrombolytic agent, Alternative Compl. Ther. 8 (3) (2002) 157–164.
[22] X. Zhou, L. Liu, X. Zeng, Research progress on the utilisation of embedding technology and suitable delivery systems for improving the bioavailability of nattokinase: a review, Food Struct. 30 (2021) 100219.
[23] L. Cao, F. Kou, M. Zhang, X. Jin, C. Ren, G. Yu, Y. Zhang, M. Wang, Effect of exogenous melatonin on the quality of soybean and natto products under drought stress, J. Chem. 2021 (2021) 1–8.
[24] J.G. Arámburo-Gálvez, A.A. Arvizu-Flores, F.I. Cárdenas-Torres, F. Cabrera-Chávez, G.I. Ramírez-Torres, L.K. Flores-Mendoza, P.E. Gastelum-Acosta, O. G. Figueroa-Salcido, N. Ontiveros, Prediction of ACE-I inhibitory peptides derived from chickpea (Cicer arietinum L.): in silico assessments using simulated enzymatic hydrolysis, molecular docking and ADMET evaluation, Foods 11 (11) (2022) 1576.
[25] T.İ. Horuz, K.B. Belibağlı, Nanoencapsulation by electrospinning to improve stability and water solubility of carotenoids extracted from tomato peels, Food Chem. 268 (2018) 86–93.
[26] P. Mudgil, W.N. Baba, H. Kamal, R.J. FitzGerald, H.M. Hassan, M.A. Ayoub, C.Y. Gan, S. Maqsood, A comparative investigation into novel cholesterol esterase and pancreatic lipase inhibitory peptides from cow and camel casein hydrolysates generated upon enzymatic hydrolysis and in-vitro digestion, Food Chem. 367 (2022) 130661.
[27] H. Xiang, S. Waterhouse, P. Liu, G.I.N. Waterhouse, J. Li, C. Cui, Pancreatic lipase-inhibiting protein hydrolysate and peptides from seabuckthorn seed meal: preparation optimization and inhibitory mechanism, Lwt 134 (2020).
[28] L. Siow, B. Choi, Y. Gan, Structure–activity studies of protease activating, lipase inhibiting, bile acid binding and cholesterol-lowering effects of pre-screened cumin seed bioactive peptides, J. Funct. Foods 27 (2016) 600–611.
[29] W. Schreiner, R. Karch, B. Knapp, N. Ilieva, Relaxation Estimation of RMSD in Molecular Dynamics Immunosimulations, Computational and Mathematical Methods in Medicine 2012, 2012.
[30] M. Arnittali, A.N. Rissanou, V. Harmandaris, Structure of biomolecules through molecular dynamics simulations, Procedia Comput. Sci. 156 (2019) 69–78.
[31] J. Vora, S. Patel, M. Athar, S. Sinha, M.T. Chhabria, P.C. Jha, N. Shrivastava, Pharmacophore modeling, molecular docking and molecular dynamics simulation for screening and identifying anti-dengue phytocompounds, J. Biomol. Struct. Dyn. 38 (6) (2020) 1726–1740.
[32] Y.-w. Dong, M.-l. Liao, X.-l. Meng, G.N. Somero, Structural flexibility and protein adaptation to temperature: molecular dynamics analysis of malate dehydrogenases of marine molluscs, Proc. Natl. Acad. Sci. USA 115 (6) (2018) 1274–1279.
[33] A.A. Zaki, A. Ashour, S.S. Elhady, K.M. Darwish, A.A. Al-Karmalawy, Calendulaglycoside A showing potential activity against SARS-CoV-2 main protease: molecular docking, molecular dynamics, and SAR studies, Journal of traditional and complementary medicine 12 (1) (2022) 16–34.
[34] L. Zhang, P. Wang, Z. Yang, F. Du, Z. Li, C. Wu, A. Fang, X. Xu, G. Zhou, Molecular dynamics simulation exploration of the interaction between curcumin and myosin combined with the results of spectroscopy techniques, Food Hydrocolloids 101 (2020) 105455.
[35] L.A. Dahabiyeh, Y. Bustanji, M.O. Taha, The herbicide quinclorac as potent lipase inhibitor: discovery via virtual screening and in vitro/in vivo validation, Chem. Biol. Drug Des. 93 (5) (2019) 787–797.
[36] J. Zhang, L. Xiao, Y. Yang, Z. Wang, G. Li, Lignin binding to pancreatic lipase and its influence on enzymatic activity, Food Chem. 149 (2014) 99–106.